chemosensors

MDPI

Article

Fabrication and Magneto-Structural Properties of Co_2-Based Heusler Alloy Glass-Coated Microwires with High Curie Temperature

Mohamed Salaheldeen [1,2,3,4], Alfonso Garcia-Gomez [1,2,4], Mihail Ipatov [1,2,4], Paula Corte-Leon [1,2,4], Valentina Zhukova [1,2,4], Juan Maria Blanco [2,4] and Arcady Zhukov [1,2,4,5,*]

1 Departamento de Polímeros y Materiales Avanzados, Facultad Química, Universidad del País Vasco, UPV/EHU, 20018 San Sebastián, Spain; mohamed.salaheldeenmohamed@ehu.eus (M.S.); alfonso.garciag@ehu.eus (A.G.-G.); mihail.ipatov@ehu.eus (M.I.); paula.corte@ehu.eus (P.C.-L.); valentina.zhukova@ehu.eus (V.Z.)
2 Departamento de Física Aplicada, EIG, Universidad del País Vasco, UPV/EHU, 20018 San Sebastián, Spain; juanmaria.blanco@ehu.eus
3 Physics Department, Faculty of Science, Sohag University, Sohag 82524, Egypt
4 EHU Quantum Center, University of the Basque Country, UPV/EHU, 48940 Leioa, Spain
5 IKERBASQUE, Basque Foundation for Science, 48011 Bilbao, Spain
* Correspondence: arkadi.joukov@ehu.eus

Abstract: In this work, we were able to produce Co_2FeSi Heusler alloy glass-covered microwires with a metallic nucleus diameter of about 4.4 μm and total sample diameter of about 17.6 μm by the Taylor–Ulitovsky Technique. This low cost and single step fabrication process allowed the preparation of up to kilometers long glass-coated microwires starting from a few grams of high purity inexpensive elements (Co, Fe and Si), for a wide range of applications. From the X-ray diffraction, XRD, analysis of the metallic nucleus, it was shown that the structure consists of a mixture of crystalline and amorphous phases. The single and wide crystalline peak was attributed to a $L2_1$ crystalline structure (5.640 Å), with a possible *B2* disorder. In addition, nanocrystalline structure with an average grain size, D_g = 17.8 nm, and crystalline phase content of about 52% was obtained. The magnetic measurements indicated a well-defined magnetic anisotropy for all ranges of temperature. Moreover, soft magnetic behavior was observed for the temperature measuring range of 5–1000 K. Strong dependence of the magnetic properties on the applied magnetic field and temperature was observed. Zero field cooling and field cooling magnetization curves showed large irreversibility magnetic behavior with a blocking temperature (T_B = 205 K). The in-plane magnetization remanence and coercivity showed quite different behavior with temperature, due to the existence of different magnetic phases induced from the internal stress created by the glass-coated layer. Moreover, a high Curie temperature was reported ($T_c \approx$ 1059 K), which predisposes this material to being a suitable candidate for high temperature spintronic applications.

Keywords: Heusler alloys; glass-coated microwires; magnetic properties; Curie temperature; X-ray diffraction

Citation: Salaheldeen, M.; Garcia-Gomez, A.; Ipatov, M.; Corte-Leon, P.; Zhukova, V.; Blanco, J.M.; Zhukov, A. Fabrication and Magneto-Structural Properties of Co_2-Based Heusler Alloy Glass-Coated Microwires with High Curie Temperature. *Chemosensors* **2022**, *10*, 225. https://doi.org/10.3390/chemosensors10060225

Academic Editor: Marco Frasconi

Received: 6 April 2022
Accepted: 13 June 2022
Published: 14 June 2022

1. Introduction

Recently, half-metallic Heusler alloys (HMHSs) have been suggested as promising candidates for next generation spintronic devices because of their extraordinary magnetic properties at a wide range of temperatures, as reported and discussed elsewhere [1,2]. This extraordinary magnetic behavior can be explained by the unique structural features of energy bands for the spin up/down states near to the Fermi energy levels. Whereas the spin up band indicates the metallic character of HMHS, the spin down band shows a semiconductor-like gap at the Fermi energy levels [3,4]. Thus, there is a complete spin

polarization (near to 100%) of the conduction electrons at the Fermi level position, as confirmed elsewhere [5–10].

Co_2-based full/half-Heusler compounds with high Curie temperature (T_c > 1100 K), high magnetic moment (~6 μ_B/f.u.), unique electronic structure and low Gilbert damping constant (α = 0.004) are the most promising materials for multi-function applications [11–13]. Moreover, unique exotic transport properties and a large anomalous Hall effect have been reported on Co_2-based Heusler alloys, due to the large Berry curvature linked with their band structure [1,2]. Thus, Co_2-based Heusler alloys are attracting the attention of the scientific community.

Generally, the $L2_1$ structure determines the physical properties of Co_2-based Heusler alloys [13,14]. Although the $L2_1$ structure is a highly ordered structure, the existence of disordered structure phases, such as B2, *A2* and *DO3*, may arise during the fabrication process of alloys [9,15]. Therefore, Co_2-based Heusler alloys are very sensitive to fabrication techniques. Thus, these kinds of alloys are widely investigated by using different fabrication processes [16–23].

The most well-known technique to prepare HMHS in different forms is arc melting for the primary bulk alloy, followed by thermal treatment under different conditions [24,25]. The physical properties of HMHS can be strongly enhanced by applying the miniaturization process where an increasing surface-to-volume ratio works to enhance the magnetic cooling applications and heat-exchange [26]. Thus, there is an urgent demand for novel fabrication methods allowing the preparation of low-dimensional materials from Heusler alloys, such as nanoparticles, thin films and thin microwires [17,27–29]. Many of these fabrication techniques are still facing challenges, such as the high cost of preparation techniques, the long period required for additional thermal treatment, chemical composition inhomogeneity, lattice mismatch between the alloy and the substrate, easy oxidation and the perspective of proper atomic ordering [29–31]. To avoid these disadvantages, alternative rapid quenching production of the Heusler alloys has recently been carried out [4,7].

The Taylor-Ulitovsky technique, involving rapid melt quenching, is suitable for preparation of thin glass-coated magnetic microwires (G-CMMWs). This technique offers low cost and fast production of thin metallic microwires, without the need for additional dimensionality reduction processes or long thermal treatments [32–38]. Recently, rapidly quenched low-dimensional nanocrystalline and amorphous materials gained special interest, due to their promising mechanical properties, excellent magnetic properties and magneto-transport properties [35,36,39–42].

Amorphous and nanocrystalline rapidly quenched materials can present unique combinations of magnetic properties, such as extremely fast domain wall propagation or giant magnetoimpedance effect [36,37,39–44]. One of the most relevant factors of these rapid quenching materials is the possibility to tailor the microstructure of the quenched alloys by controlling different parameters, such as the quenching rate, the chemical composition and the melting temperature of the selected alloy, and its phase diagram [35]. One of the main advantages of this technology is that it is suitable for fast (hundreds of meters per minute) fabrication of rather long and continuous metallic microwires (up to several kilometers long) with the widest possible diameter range (by four orders of magnitude, i.e., from 0.1 to 100 μm), covered with insulating and flexible glass-coating [28,31,33–36,43–45]. In addition, the existence of flexible, thin, highly transparent and insulating glass coating works on improving mechanical and biocompatibility properties, which opens the door for the biomedical application of the G-CMMWs [46–48]. Finally, by the single-step method, with a high quenching rate, it is possible to produce microwires from Heusler alloys with single crystalline phase and well-defined magnetic anisotropy [4,7,33–36,49,50]. Therefore, the Co_2-based Heusler G-CMMWs represent a promising smart metamaterial for multi-functional application for a new generation of spintronic devices.

In the current study we present the basic structural and magnetic characterization of Co_2FeSi G-CMMWs fabricated by the Taylor-Utilovsky method to illustrate their possible application in advanced spintronic devices.

2. Materials and Methods

Full Heusler alloy with nominal composition of $Co_{50}Fe_{25}Si_{25}$ was prepared by the arc melting technique from pure metals, Co (99.99%), Fe (99.99%) and Si (99.9%), in argon atmosphere to prevent oxide formation during the melting process. The repetition of the melting process was done several times to improve homogeneity of the alloy. Magnetic glass-coated microwires were fabricated by the Taylor-Ulitovsky technique, which consisted of drawing and casting directly from the melted $Co_{50}Fe_{25}Si_{25}$ alloy, as described in detail elsewhere [33,36–38,51–56]. Briefly, an ingot was heated above its melting point by a high frequency inductor, then a glass capillary was formed, which was filled with molten alloy, drawn out and wound onto a rotating pick-up bobbin [33,35,36]. The diameter of the metallic nucleus, d, could be controlled by the speed at which the wire was drawn and the velocity of the rotation of the pick-up bobbin [35,36]. Rapid melt quenching was achieved by a stream of coolant when the formed microwire passed through a coolant stream [35,36]. The metallic nucleus diameter, d, of prepared $Co_{50}Fe_{25}Si_{25}$ microwire was about 4 ($d = 4.4 \pm 0.1$) μm, while the total diameter was $D = 17.6 \pm 0.1$ μm.

One of the peculiarities of the glass-coated microwire fabrication process is that the metallic nucleus is surrounded by the glass coating during the rapid solidification process. Such a process is associated with elevated internal stresses arising from rapid quenching itself, drawing and from the different thermal expansion coefficients of the glass and the metallic nucleus [33,34,36,38].

We checked the chemical composition and the homogeneity of the Co_2FeSi G-CMWs by using Energy Dispersive X-ray/Scanning Electron Microscopy (EDX/SEM). By analyzing the EDX data of Co_2FeSi G-CMWs in different parts of the microwire we found that the alloy showed a perfect chemical composition wherein Co, Si, and Fe elements were well distributed with the same nominal percentage at the different parts of the microwire, as illustrated in Figure 1.

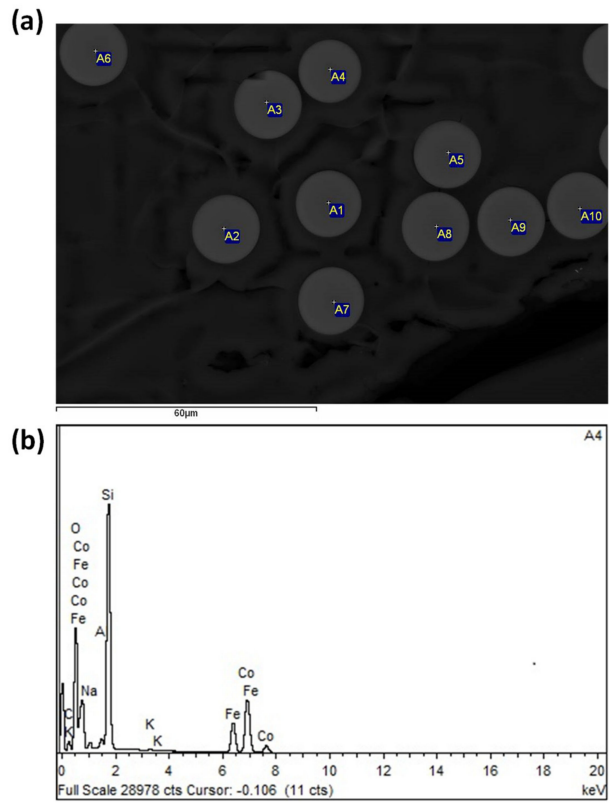

Figure 1. The cross section of Co_2FeSi G-CMMWs images (**a**) and the chemical composition spectra of EDX at one of the points (**b**).

The microstructure and its possible induced phase analysis were investigated by means of X-ray diffraction (XRD) BRUKER (D8 Advance, Bruker AXS GmbH, Karlsruhe, Germany). Cu K_α (λ = 1.54 Å) radiation was used in all the patterns.

The investigation of the magnetic properties of Co_2FeSi G-CMWs was performed by using the Physical Property Magnetic System, PPMS (Quantum Design Inc., San Diego, CA, USA) for the field cooling, field heating and zero-field cooling magnetization curves for a temperature range from 5–400 K, with an applied external magnetic field of 50 Oe and 50 kOe. For the Curie temperature evaluation, we used a Vibrating Sample Magnetometer (VSM) at temperatures from 400 K to 1000 K, with applied low magnetic field (H = 50 Oe).

3. Results and Discussion

The morphological characterization of Co_2FeSi G-CMMWs was performed using the scanning electron microscopy technique (SEM). Figure 1a shows the perfect cylindrical cross section and homogeneous elements distribution of the Co_2FeSi G-CMMWs. To confirm the nominal composition of $Co_{50}Fe_{25}Si_{25}$ G-CMMWs, an analysis of the chemical composition of the metallic nucleus was performed using EDX, as shown in Figure 1b. From the EDX data obtained from Figure 1b the composition of the metallic nucleus was observed to be slightly different from the stoichiometric one (Co_2FeSi). This small difference was related to the peculiarities of the preparation method involving alloy melting and casting. To estimate the amount of difference we checked the nominal composition for 10 points as illustrated in Figure 1a. For all points a 2:1 ratio was confirmed for Co and Fe, respectively, with an atomic average $Co_{45}Fe_{22}Si_{33}$. A high ratio of Si was observed, due to the interfacial layer between the glass coating and the metallic nucleus. The origin of such an interfacial layer was related to the peculiarities of the preparation method involving alloy melting inside the glass tube and subsequent casting. As previously reported [45], typically the thickness of such an interfacial layer is about 0.5 μm. Accordingly, for the present case (d ≈ 4 μm) the contribution of such an interfacial layer reflected in elevated Si-content might be relevant. Thus, this explains the high signal of Si that appeared on the EDX spectra (see Figure 1b).

Figure 2 illustrates the X-ray diffraction (XRD) analysis of Co_2FeSi G-CMMWs showing a wide plateau centered on $2\theta \approx 22.5^\circ$. That peak corresponds to the amorphous phase of the glass, as we expected from the Taylor-Ulitovsky method. Along with the amorphous pattern, another peak appeared at $2\theta \approx 45.6^\circ$ related to the crystalline pattern of the Co_2FeSi metallic nucleus and corresponding to the *B2* phase, which agrees with our previous work on Co_2FeSi G-CMMWs [14].

For estimation of the average of the crystalline grain size, D_g, we performed an analysis of the width and the crystalline peak position using the Debye Scherrer equation as follows [35,41,44]:

$$D_g = K\,\lambda/\beta\,\cos 2\theta \quad (1)$$

where (K = 0.9), λ is the wave length of XRD (Cu K_α (λ = 1.54 Å)), β is the total width at half maximum of the peak and 2θ is the angular position of the peak.

The XRD pattern of the Co_2FeSi G-CMMWs sample fitted best to a mixture of cubic phase (lattice parameter a = 5.640 Å, D_g = 17.8 nm) and an amorphous phase.

After evaluation of the nanocrystalline grain size we could estimate the crystalline phase content, S, from the diffraction scan where the sum of the total peak area consisted of crystalline and amorphous diffractograms together. The crystalline phase content could be calculated from the following equation [57,58]:

$$S\,(\%) = \frac{\int q^2 I_c\, dq}{\int q^2 I\, dq} \approx \frac{\int I_c\, d(2\theta)}{\int I\, d(2\theta)} \quad (2)$$

where $q = \frac{4\pi sin\theta}{\lambda}$ and $I = I_{am} + I_c$, where I_{am} and I_c are the integrated intensity of the amorphous and the crystalline components, respectively. By calculating the total area under the peak, we could easily estimate S ≈ 64% of the Co_2FeSi G-CMMWs samples, which was related to the distribution of the grains inside the crystal.

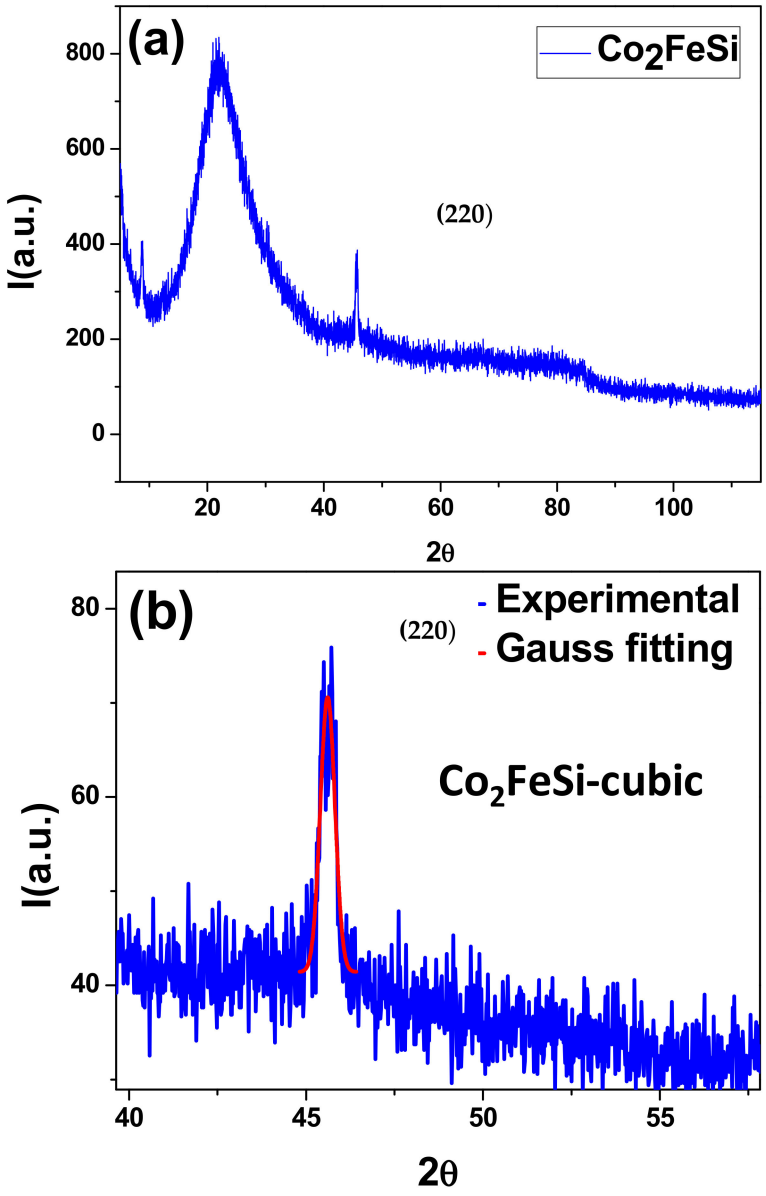

Figure 2. X-ray diffraction pattern of Co_2FeSi G-CMMWs (**a**) and focusing on the crystalline part of Co_2FeSi G-CMMWs with a Gauss fitting (**b**).

The XRD and its analysis matched with our previous studies of similar alloys, together with the chemical composition of the studied sample; which indicated the presence of the cubic Co_2FeSi phase [14,59]. According to theoretical calculations obtained from the materialsproyect.org [60], the signal (220) peak represented a highly ordered $L2_1$ cubic structure (space group: Fm-3m). The lattice parameter of Co_2FeSi was found to be 5.640 Å, which is in agreement with similar compositions [14,59].

Figure 3 shows the magnetic properties (dependencies of magnetic moment, M, versus magnetic field, H) of Co_2FeSi G-CMMWs at different temperatures, measured in an applied magnetic field between ±50 kOe, at a temperature range from 5 to 400 K. As plotted in Figure 3a,b, all M-H loops showed ferromagnetic behavior over the entire measured temperature range. The maximum values of the magnetic parameters, such as magnetic moment and magnetic remanence, M_r, were detected at 5 K and the lowest values were observed at 400 K. Additionally, all the hysteresis loops showed rectangular M-H loop shapes, similar to the behavior observed in Co_2FeSi alloys deposited by different techniques and in different forms [12,14,17,29,61]. For the temperature range from 200 K to 400 K the

hysteresis loops showed low saturation field, H_s, anisotropy field, H_k, M_r and H_c values, as indicated in Figure 3b.

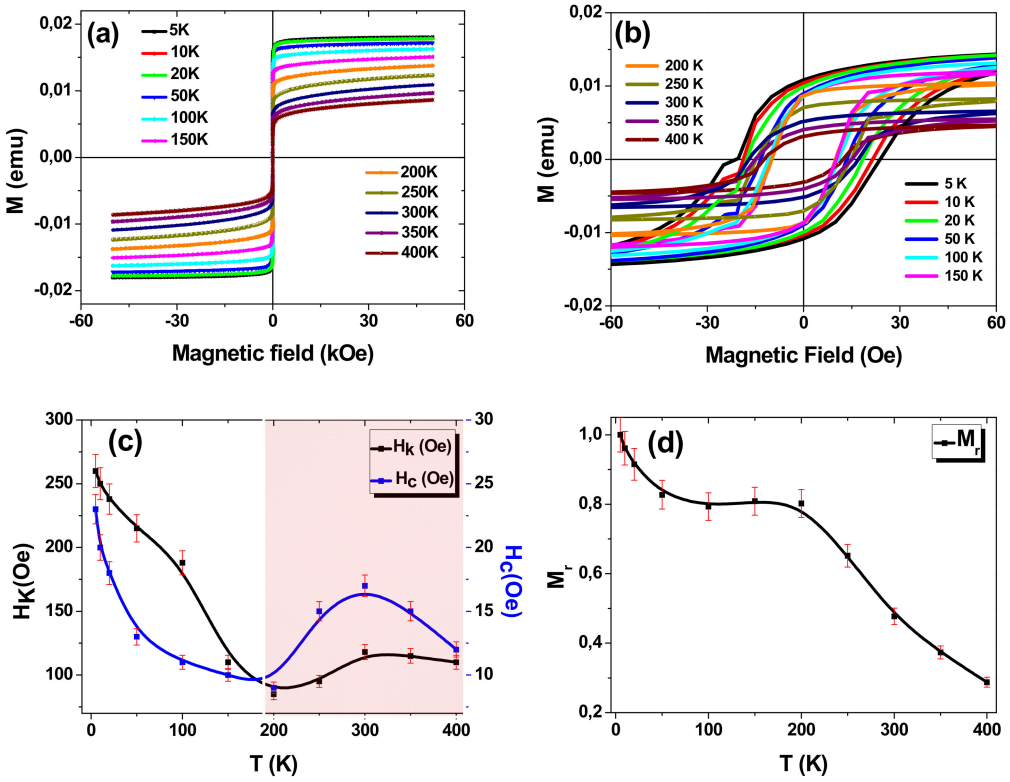

Figure 3. (**a**) Hysteresis loops, measured in magnetic field applied parallel to the axis of microwires in the temperature range from 5 to 400 K for as prepared Co_2FeSi G-CMMWs, and measured magnetic field between ±50 kOe and (**b**) hysteresis loops with low scale magnetic field. (**c**,**d**) temperature dependence of the coercivity and anisotropy field and normalized remanence, respectively, for Co_2FeSi G-CMMWs (lines for eye guide).

The structure consisted of a mixture of the amorphous and the crystalline phases. Accordingly, in such kinds of samples with mixed structure it was very difficult to evaluate the anisotropy constant. In the present case, we evaluated the magnetic anisotropy field, H_k (provided in Figure 3c together with H_c) from the hysteresis loops presented in Figure 3a,b.

It is worth noting that such almost rectangular hysteresis loops have been previously reported, not only in completely amorphous microwires and thin films [36,62], but also in microwires with mixed amorphous-crystalline and nanocrystalline microwires [41,55]. Such hysteresis loops can be related to shape magnetic anisotropy, as well as to the axial character of internal stresses induced by the difference in the thermal expansion coefficients of the metallic nucleus and glass-coating.

As discussed above, there are three main sources of internal stresses, σ_i, in glass-coated microwires: the difference in thermal expansion coefficients of the metallic alloy and glass, the quenching internal stresses, related to the rapid solidification of metallic alloy, and drawing stresses [33,34,36–38,49]. The origin of the quenching internal stresses in microwires is related to the solidification of the metallic alloy from the surface towards the wire axis. The common approach for evaluation of such internal stress components, consists of consideration of the successive concentric cylindrical shells solidifying consecutively, starting from outside, due to the temperature gradient at the glass transition temperature [34,38,43]. We theoretically predicted and experimentally confirmed that the largest internal stresses were those related to the difference in thermal expansion coefficients of the metallic alloy and glass: the σ_i value up to 4 GPa [33,34,36–38,49]. Additionally, the axial σ_i component,

σ_z, was the largest one, affected by the ρ-ratio given as d/D, as followed from the most simplified approximation, σ_i given as [36–38]:

$$\sigma_\varphi = \sigma_r = \mathrm{P} = \varepsilon \mathrm{Ek}\Delta/(\mathrm{k}/3 + 1)\Delta + 4/3; \sigma_z = \mathrm{P}(\mathrm{k} + 1)\Delta + 2/(\mathrm{k}\Delta + 1) \quad (3)$$

where σ_φ and σ_r are circular and radial stresses respectively, $\Delta = (1 - \rho^2)/\rho^2$, k $= E_g/E_m$, E_m, E_g—Young modulus of metallic nucleus and glass, respectively, $\varepsilon = (\alpha_m - \alpha_g)(T_m - T_{room})$, α_m, α_g are thermal expansion coefficients of metallic nucleus and glass, respectively, and T_m, T_{room} are melting and room temperatures.

Accordingly, the axial magnetic anisotropy observed in the studied microwire must have been related to the axial character of the internal stresses together with the high and positive magnetostriction coefficient, λ_s, of Co-Fe based alloys [36–38].

Generally, Co_2-based Heusler alloy thin wires and thin films with $L2_1$ cubic structure have cubic magnetiocrystalline anisotropy besides the uniaxial magnetic anisotropy induced by the wire shape [14,62]. Therefore, the reduced M_r, H_c, H_k and H_s values could be attributed to competition between the two kinds of magnetic anisotropy for T range from 200 K to 400 K. By decreasing the temperature, the enhancement in the magnetocrystalline anisotropy is supposed to be due to increase in the saturation magnetization and degree of the ferromagnetic order [62].

By analyzing the M-H curves of Co_2FeSi G-CMMWs the coercivity, H_c, showed quite soft magnetic behavior where the lowest values of H_c = 9 Oe were detected below the room temperature (RT) at 200 K. Meanwhile, the highest value of H_c = 25 Oe was observed at T = 5 K with a difference around 16 Oe. In addition, the anisotropy field, H_k, showed the lowest value at 200 K and the highest value at 5 K. Quite unusual behavior of H_c and H_k was detected (see Figure 3c). Where H_c and H_k first increased with decreasing temperature from 400 K to 300 K, they then started decreasing over the range of T from 300 K to 200 K. Finally, H_c and H_k increased with decreasing T and reached a maximum at T = 5 K. Such anomalous magnetic behavior of H_c and H_k has not been reported in Co_2FeSi with different forms. This behavior of H_c and H_k was due to the internal stresses, originating in the glass coating. Such stresses are strongly affected by the temperature and change in the magnetic phase with T. As reported in previous studies, and discussed above, the internal stresses, induced during the preparation of the microwires, are mostly related to the difference in the thermal expansion of the metallic nucleus and the glass layer [38–43,52]. The presence of such stresses can induce a modification in the micromagnetic, and even crystalline, structure of glass-coated microwires, and this strongly effects the values and behavior of H_c and H_k [38,49]. The normalized values of M_r to the highest values of magnetic moment at 5 K (i.e., $M_r = M/M_{5K}$) showed a regular magnetic behavior with temperature, as plotted in Figure 3d. The M_r sharply increased from 0.28 to 0.81 by decreasing the temperature from 400 K to 200 K, respectively. Then, semi stable values of M_r were observed at T range from 200 K to 100 K. Finally, below 100 K the M_r started to increase with decreasing T until it reached a maximum at 5 K. The behavior of M_r and H_c with temperature confirmed the sensitivity of the magnetic behavior of Co_2FeSi G-CMMWs to temperature. The anomalous magnetic behavior of H_c and H_k, beside the usual behavior of M_r with temperature, confirmed the sensitivity of these micro magnetic systems and could open the door for alternative studies investigating the impact of annealing and the geometric parameters which pave the way for using Co_2FeSi G-CMMWs in designing spintronic devices based on thermo-magnetic switching.

It is important to understand that the thermal stability of the ferromagnetic materials is an extremely important property concerning its potential use in spintronic devices in order to operate at/below or above RT. Thus, we measured the magnetization dependence on temperature (M vs. T), i.e., zero field cooling, ZFC, field cooling, FC, and field heating, FH, at low magnetic field (H = 50 Oe) and high magnetic field (H = 50 kOe) and temperature range from 4 to 1000 K, as indicated in Figure 4. We normalized the M vs. T curves to the maximum values of magnetic moment at 5 K to better compare. In FC protocol, the Co_2FeSi G-CMMWs was cooled down to 4 K under an applied magnetic field, which

caused the random magnetic moment vectors to freeze parallel to the applied field at low temperatures. The magnetic moments show random orientation in the ZFC system at equilibrium. By increasing the temperature in a low static magnetic field, the magnetic moments follow the direction of applied external magnetic field and the magnetization increases if the relaxation phenomena are neglected. Moreover, for further increase of temperature, the relaxation becomes progressively more prominent and, as a result, above a certain temperature, ZFC decreases and finally equals FC [63]. In our current study the ZFC and FC magnetic curve showed large magnetic irreversibility at low magnetic field i.e., H = 50 Oe, with a blocking temperature, T_B, of about 205 K, as shown in Figure 4a. Such irreversibility behavior disappeared by applying a high magnetic field (see Figure 4b), i.e., this behavior strongly depends on the magnitude of the applied magnetic field. The mentioned irreversibility behavior in magnetic materials at applied low magnetic field is due to the coexistence of typical re-entrant ferromagnetism and spin glass-type behavior, as reported elsewhere [64]. In addition, the disordered structure and chemical composition of Co_2FeSi G-CMMWs affects the irreversibility behavior where the magnetic ground state is not purely ferromagnetic and random spin disorder (*B2* phase) is also found with the ferromagnetic order ($L2_1$ phase) [63,64]. This behavior is related to the internal stress of glass coating during the fabrication process which induces a disordered structure phase (*B2*) beside the ordered one ($L2_1$), and amorphous one (as described in the XRD analysis). By increasing the applied magnetic field (50 kOe) the *B2* phase was frustrated and the irreversibility behavior disappeared.

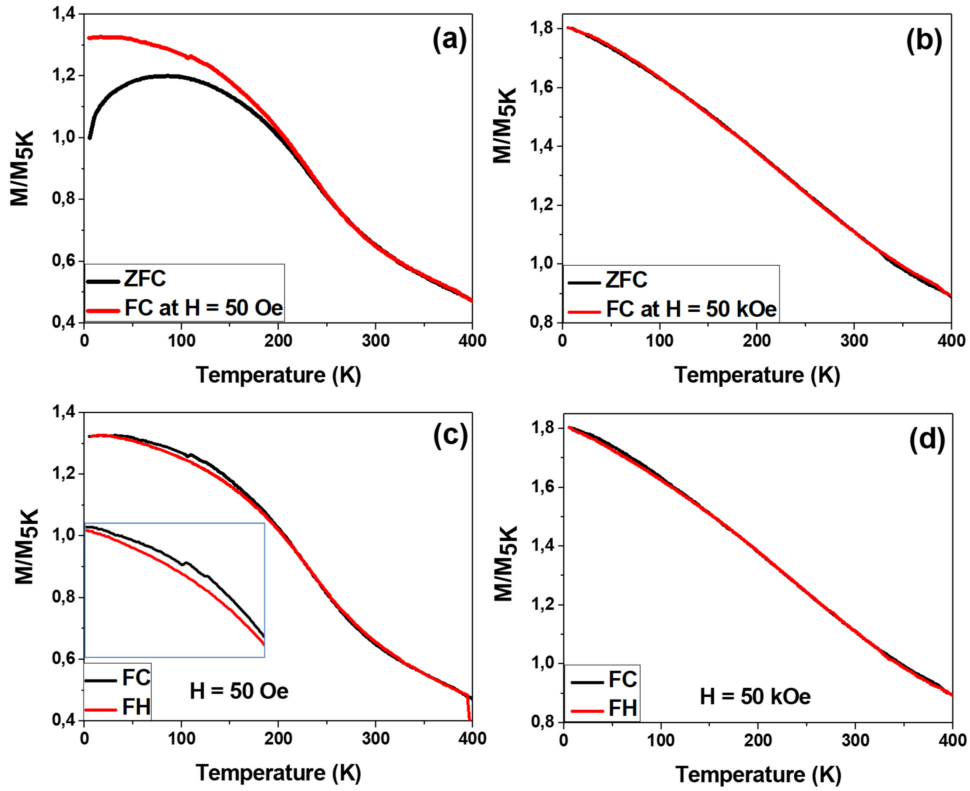

Figure 4. (**a**,**b**) Zero field cooling (ZFC), field cooling (FC) of Co_2FeSi G-CMMWs at temperature range 400 K to 5 K with different applied magnetic field low field 50 Oe and high magnetic field 50 kOe, respectively. (**c**,**d**) FC from 400 K to 5 K and field heating (FH) from 5 K to 400 K of Co_2FeSi G-CMMWs with different applied magnetic field low field 50 Oe and high magnetic field 50 kOe, respectively.

To check the possible magnetic phase transition with changes of temperature, the FC and FH curves were measured at low and high magnetic field. As described in Figure 4c, the FC and FH curves with applied low magnetic field (H = 50 Oe) were perfectly matching in the temperature range from 400 to 190 K, which indicated a perfectly stable ferromagnetic

state in this range of T. Below T = 190 K a small spacing between FC and FH was detected and FC ascended the FH curves then matched again at T = 15 K. This behavior is due to a magnetic phase transition, as described and reported elsewhere [4,29,65–67]. Such behavior was not observed when the FC and FH were measured at high magnetic fields, as illustrated in Figure 4d. It is noteworthy, that the changing of magnetic behavior of H_c and M_r occurred for the temperature below 200 K i.e., below T_B. Thus, the behavior of H_c and M_r was strongly related to the changing of the magnetic phase transition where a different magnetic response was found.

To examine the magnetic behavior of Co_2FeSi G-CMMWs at high temperature, FC and FH at low magnetic field (H = 50 Oe) and temperature range from 400 to 1000 K was performed, as indicated in Figure 5.

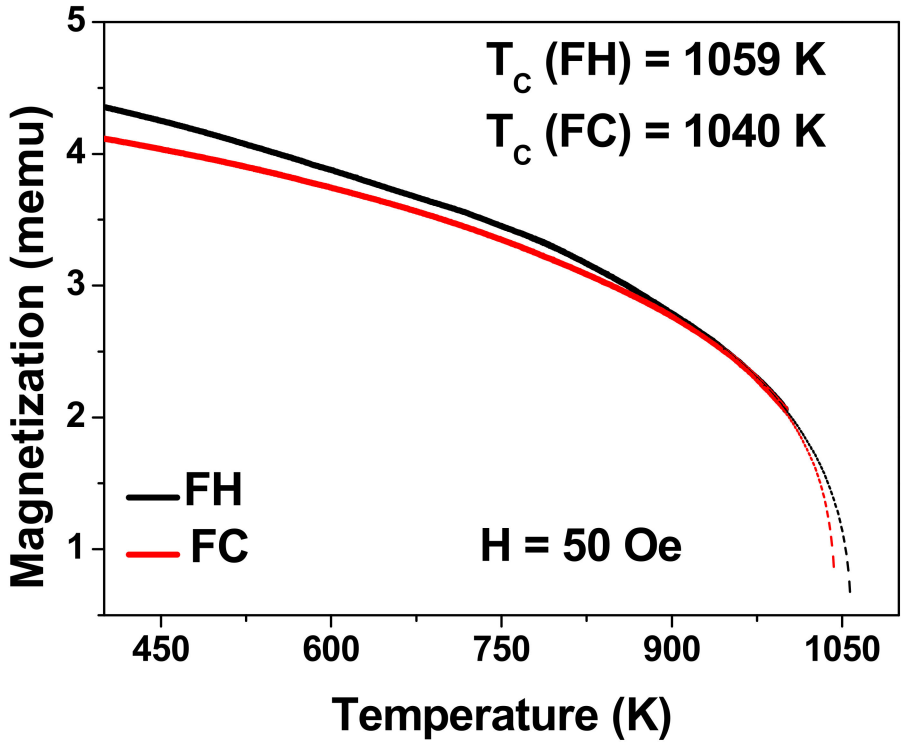

Figure 5. Temperature dependence of magnetization measured for Co_2FeSi G-CMMWs at applied magnetic field (50 Oe) and temperature range from 400 to 1000 K. Dashed black and red lines refer to the T_C fitting curves.

As shown in Figure 5, FC and FH magnetization curves showed the ordinary ferromagnetic behavior—magnetization decreased with increase of temperature. FC and FH magnetic curves showed different behavior for the temperature range from 400 to 900 K. Above T = 900 K the two magnetic curves were perfectly matching. Below the blocking temperature a magnetic phase transition was found. Unfortunately, we were not able to observe the T_C of Co_2FeSi G-CMMWs, as it is expected to be more than 1100 K for the bulk alloy. Therefore, a fitting of FC and FH magnetic curves was performed by using the following equation ($M(H,T) = M_0 \frac{T_c - T}{T_c}$) and the estimation of T_C = 1040 K and 1059 K for FC and FH magnetic curves, respectively, and it corresponded well with the value from the literature [13]. The differences in the T_C values must be related to different magnetic phases where the magnetic responses are different.

4. Conclusions

We have reported fabrication and magneto-structural characterization of Co_2FeSi G-CMMWs prepared by the Taylor-Ulitovsky technique. From the XRD analysis, it was found that the studied microwires had mixed amorphous-crystalline structure. The XRD

analysis illustrated the formation of ordered ($L2_1$) and disordered ($B2$) structure phases. Well-defined magnetic anisotropy parallel to the axis of the Co_2FeSi G-CMMWs was observed. The thermo-magnetic behavior of Co_2FeSi G-CMMWs, with temperature ranging from 5 to 1000 K, was investigated. ZFC-FC magnetic curves showed a large irreversibility magnetic behavior with a blocking temperature at 205 K. A strong dependence of the thermo-magnetic properties, as a function of magnetic field and temperature, was confirmed. Different tendencies of H_c, H_k and M_r were detected below and above the blocking temperature. Finally, a high Curie temperature (1059 K) was reported. Future research is necessary to explain the effects of annealing conditions and geometrical parameters on the magneto-structural and thermoelectric properties. These observations will open an approach to the use of Co_2FeSi G-CMMWs with unusual magnetization behavior, especially in terms of changing the micromagnetic and magnetic phase and structure for the design of spintronic devices based on thermo-magnetic switching.

Author Contributions: Conceptualization, M.S. and A.Z.; methodology, M.I. and A.G.-G.; validation, M.S., V.Z. and A.Z.; formal analysis, M.S. and A.G.-G.; investigation, M.S., A.Z., V.Z., P.C.-L., A.G.-G. and J.M.B.; resources, V.Z. and A.Z.; data curation, M.I.; writing—original draft preparation, M.S. and A.Z.; writing—review and editing, M.S. and A.Z.; visualization, M.S. and A.G.-G.; supervision, A.Z.; project administration, V.Z. and A.Z.; funding acquisition, V.Z. and A.Z. All authors have read and agreed to the published version of the manuscript.

Funding: This research was funded by the Spanish MCIU, under PGC2018-099530-B-C31 (MCIU/AEI/FEDER, UE), by EU under "INFINITE" (HORIZON-CL5-2021-D5-01-06) project, by the Government of the Basque Country under PUE_2021_1_0009 and Elkartek (MINERVA, ZE-KONP and COMPONENS) projects, by the University of the Basque Country, under the scheme of "Ayuda a Grupos Consolidados" (Ref.: GIU18/192) and under the COLAB20/15 project and by the Diputación Foral de Gipuzkoa in the frame of Programa "Red guipuzcoana de Ciencia, Tecnología e Innovación 2021" under 2021-CIEN-000007-01 project.

Institutional Review Board Statement: Not applicable.

Informed Consent Statement: Not applicable.

Data Availability Statement: Not applicable.

Acknowledgments: The authors are thankful for the technical and human support provided by SGIker of UPV/EHU (Medidas Magnéticas Gipuzkoa) and European funding (ERDF and ESF). We wish to thank the administration of the University of the Basque Country, which not only provides very limited funding, but even expropriates the resources received by the research group from private companies for the research activities of the group. Such interference helps keep us on our toes.

Conflicts of Interest: The authors declare no conflict of interest.

References

1. Li, P.; Koo, J.; Ning, W.; Li, J.; Miao, L.; Min, L.; Zhu, Y.; Wang, Y.; Alem, N.; Liu, C.X.; et al. Giant Room Temperature Anomalous Hall Effect and Tunable Topology in a Ferromagnetic Topological Semimetal Co_2MnAl. *Nat. Commun.* **2020**, *11*, 3476. [CrossRef] [PubMed]
2. Belopolski, I.; Manna, K.; Sanchez, D.S.; Chang, G.; Ernst, B.; Yin, J.; Zhang, S.S.; Cochran, T.; Shumiya, N.; Zheng, H.; et al. Discovery of Topological Weyl Fermion Lines and Drumhead Surface States in a Room Temperature Magnet. *Science* **2019**, *365*, 1278–1281. [CrossRef] [PubMed]
3. Li, J.; Meng, F.; Liu, G.; Chen, X.; Hongzhi, L.; Liu, E.; Wu, G. Electronic Structure and Magnetism of Binary Fe-Based Half-Heusler Alloys Fe2Z (Z=In, Sn, Sb and As). *J. Magn. Magn. Mater.* **2013**, *331*, 82–87. [CrossRef]
4. Zhukova, V.; Chernenko, V.; Ipatov, M.; Zhukov, A. Magnetic Properties of Heusler-Type NiMnGa Glass-Coated Microwires. *IEEE Trans. Magn.* **2015**, *51*, 2501604. [CrossRef]
5. Manna, K.; Sun, Y.; Muechler, L.; Kübler, J.; Felser, C. Heusler, Weyl and Berry. *Nat. Rev. Mater.* **2018**, *3*, 244–256. [CrossRef]
6. Nayak, A.K.; Nicklas, M.; Chadov, S.; Khuntia, P.; Shekhar, C.; Kalache, A.; Baenitz, M.; Skourski, Y.; Guduru, V.K.; Puri, A.; et al. Design of Compensated Ferrimagnetic Heusler Alloys for Giant Tunable Exchange Bias. *Nat. Mater.* **2015**, *14*, 679–684. [CrossRef]
7. Varga, R.; Ryba, T.; Vargova, Z.; Saksl, K.; Zhukova, V.; Zhukov, A. Magnetic and Structural Properties of Ni-Mn-Ga Heusler-Type Microwires. *Scr. Mater.* **2011**, *65*, 703–706. [CrossRef]

8. De Groot, R.A.; Mueller, F.M.; Engen, P.G.V.; Buschow, K.H.J. New Class of Materials: Half-Metallic Ferromagnets. *Phys. Rev. Lett.* **1983**, *50*, 2024. [CrossRef]
9. Makinistian, L.; Faiz, M.M.; Panguluri, R.P.; Balke, B.; Wurmehl, S.; Felser, C.; Albanesi, E.A.; Petukhov, A.G.; Nadgorny, B. On the Half-Metallicity of Co_2FeSi Heusler Alloy: Point-Contact Andreev Reflection Spectroscopy and Ab Initio Study. *Phys. Rev. B-Condens. Matter Mater. Phys.* **2013**, *87*, 220402. [CrossRef]
10. Wüstenberg, J.P.; Cinchetti, M.; Sánchez Albaneda, M.; Bauer, M.; Aeschlimann, M. Spin- and Time-Resolved Photoemission Studies of Thin Co_2FeSi Heusler Alloy Films. *J. Magn. Magn. Mater.* **2007**, *316*, e411–e414. [CrossRef]
11. Galanakis, I.; Dederichs, P.H.; Papanikolaou, N. Slater-Pauling Behavior and Origin of the Half-Metallicity of the Full-Heusler Alloys. *Phys. Rev. B* **2002**, *66*, 174429. [CrossRef]
12. Hazra, B.K.; Kaul, S.N.; Srinath, S.; Raja, M.M. Uniaxial Anisotropy, Intrinsic and Extrinsic Damping in Co_2FeSi Heusler Alloy Thin Films. *J. Phys. D. Appl. Phys.* **2019**, *52*, 325002. [CrossRef]
13. Wurmehl, S.; Fecher, G.H.; Kandpal, H.C.; Ksenofontov, V.; Felser, C.; Lin, H.J.; Morais, J. Geometric, Electronic, and Magnetic Structure of Co_2FeSi: Curie Temperature and Magnetic Moment Measurements and Calculations. *Phys. Rev. B Condens. Matter Mater. Phys.* **2005**, *72*, 184434. [CrossRef]
14. Galdun, L.; Ryba, T.; Prida, V.M.; Zhukova, V.; Zhukov, A.; Diko, P.; Kavečanský, V.; Vargova, Z.; Varga, R. Monocrystalline Heusler Co_2FeSi Alloy Glass-Coated Microwires: Fabrication and Magneto-Structural Characterization. *J. Magn. Magn. Mater.* **2018**, *453*, 96–100. [CrossRef]
15. Romaka, V.; Omar, A.; Löser, W.; Büchner, B.; Wurmehl, S. Thermodynamic and DFT Modeling in Quaternary Co-Based Heusler Phase Space: Understanding the Interplay between Disorder, Bonding, and Magnetism. *Comput. Mater. Sci.* **2022**, *203*, 111089. [CrossRef]
16. Leiva, L.; Granville, S.; Zhang, Y.; Dushenko, S.; Shigematsu, E.; Shinjo, T.; Ohshima, R.; Ando, Y.; Shiraishi, M. Giant Spin Hall Angle in the Heusler Alloy Weyl Ferromagnet Co_2MnGa. *Phys. Rev. B* **2021**, *103*, L041114. [CrossRef]
17. Boehnke, A.; Martens, U.; Sterwerf, C.; Niesen, A.; Huebner, T.; Von Der Ehe, M.; Meinert, M.; Kuschel, T.; Thomas, A.; Heiliger, C.; et al. Large Magneto-Seebeck Effect in Magnetic Tunnel Junctions with Half-Metallic Heusler Electrodes. *Nat. Commun.* **2017**, *8*, 1626. [CrossRef]
18. Karim, M.R.; Adhikari, A.; Panda, S.N.; Sharangi, P.; Kayal, S.; Manna, G.; Kumar, P.S.A.; Bedanta, S.; Barman, A.; Sarkar, I. Ultrafast Spin Dynamics of Electrochemically Grown Heusler Alloy Films. *J. Phys. Chem. C* **2021**, *125*, 10483–10492. [CrossRef]
19. Ahmad, A.; Mitra, S.; Srivastava, S.K.; Das, A.K. Size-Dependent Structural and Magnetic Properties of Disordered Co_2FeAl Heusler Alloy Nanoparticles. *J. Magn. Magn. Mater.* **2019**, *474*, 599–604. [CrossRef]
20. Yang, F.J.; Min, J.J.; Kang, Z.W.; Tu, S.Y.; Chen, H.B.; Liu, D.G.; Li, W.J.; Chen, X.Q.; Yang, C.P. The Influence of PH Value and Composition on the Microstructure, Magnetic Properties of Co-Fe-Al Heusler Nanoparticles. *Chem. Phys. Lett.* **2017**, *670*, 1–4. [CrossRef]
21. Ahmad, A.; Srivastava, S.K.; Das, A.K. First-Principles Calculations and Experimental Studies on Co_2FeGe Heusler Alloy Nanoparticles for Spintronics Applications. *J. Alloys Compd.* **2021**, *878*, 160341. [CrossRef]
22. Jirásková, Y.; Buršík, J.; Janičkovič, D.; Životský, O. Influence of Preparation Technology on Microstructural and Magnetic Properties of Fe_2MnSi and Fe_2MnAl Heusler Alloys. *Materials* **2019**, *12*, 710. [CrossRef] [PubMed]
23. Titov, A.; Jiraskova, Y.; Zivotsky, O.; Bursik, J.; Janickovic, D. Microstructure and Magnetism of Co_2FeAl Heusler Alloy Prepared by Arc and Induction Melting Compared with Planar Flow Casting. *AIP Adv.* **2017**, *8*, 047206. [CrossRef]
24. Acet, M.; Mañosa, L.; Planes, A. Magnetic-Field-Induced Effects in Martensitic Heusler-Based Magnetic Shape Memory Alloys. *Handb. Magn. Mater.* **2011**, *19*, 231–289. [CrossRef]
25. Dunand, D.C.; Müllner, P. Size Effects on Magnetic Actuation in Ni-Mn-Ga Shape-Memory Alloys. *Adv. Mater.* **2011**, *23*, 216–232. [CrossRef]
26. Kuz'min, M.D. Factors Limiting the Operation Frequency of Magnetic Refrigerators. *Appl. Phys. Lett.* **2007**, *90*, 251916. [CrossRef]
27. Nehla, P.; Ulrich, C.; Dhaka, R.S. Investigation of the Structural, Electronic, Transport and Magnetic Properties of Co2FeGa Heusler Alloy Nanoparticles. *J. Alloys Compd.* **2019**, *776*, 379–386. [CrossRef]
28. Wang, B.; Liu, Y. Exchange Bias and Inverse Magnetocaloric Effect in Co and Mn Co-Doped Ni_2MnGa Shape Memory Alloy. *Metals* **2013**, *3*, 69–76. [CrossRef]
29. Patra, N.; Prajapat, C.L.; Babu, P.D.; Rai, S.; Kumar, S.; Jha, S.N.; Bhattacharyya, D. Pulsed Laser Deposited Co_2FeSi Heusler Alloy Thin Films: Effect of Different Thermal Growth Processes. *J. Alloys Compd.* **2019**, *804*, 470–485. [CrossRef]
30. Khovaylo, V.V.; Rodionova, V.V.; Shevyrtalov, S.N.; Novosad, V. Magnetocaloric Effect in "Reduced" Dimensions: Thin Films, Ribbons, and Microwires of Heusler Alloys and Related Compounds. *Phys. Status Solidi* **2014**, *251*, 2104–2113. [CrossRef]
31. Belmeguenai, M.; Tuzcuoglu, H.; Gabor, M.S.; Petrisor, T.; Tiusan, C.; Zighem, F.; Chérif, S.M.; Moch, P. Co_2FeAl Heusler Thin Films Grown on Si and MgO Substrates: Annealing Temperature Effect. *J. Appl. Phys.* **2014**, *115*, 043918. [CrossRef]
32. Vázquez, M. Soft magnetic wires. *Phys. B* **2001**, *299*, 302–313. [CrossRef]
33. Chiriac, H.; Óvári, T.A.; Pop, G. Internal stress distribution in glass-covered amorphous magnetic wires. *Phys. Rev. B* **1995**, *52*, 10104–10113. [CrossRef] [PubMed]
34. Óvári, T.-A.; Lupu, N.; Chiriac, H. Rapidly Solidified Magnetic Nanowires and Submicron Wires. In *Advanced Magnetic Materials*; Malkinski, L., Ed.; InTech: London, UK, 2012; pp. 1–32. ISBN 978-953-51-0637-1.

35. Zhukov, A.; Ipatov, M.; Talaat, A.; Blanco, J.M.; Hernando, B.; Gonzalez-Legarreta, L.; Suñol, J.J.; Zhukova, V. Correlation of Crystalline Structure with Magnetic and Transport Properties of Glass-Coated Microwires. *Crystals* **2017**, *7*, 41. [CrossRef]
36. Zhukov, A.; Corte-Leon, P.; Gonzalez-Legarreta, L.; Ipatov, M.; Blanco, J.M.; Gonzalez, A.; Zhukova, V. Advanced Functional Magnetic Microwires for Technological Applications. *J. Phys. D Appl. Phys.* **2022**, *55*, 253003. [CrossRef]
37. Zhukova, V.; Corte-Leon, P.; Blanco, J.M.; Ipatov, M.; Gonzalez-Legarreta, L.; Gonzalez, A.; Zhukov, A. Development of Magnetically Soft Amorphous Microwires for Technological Applications. *Chemosens* **2022**, *10*, 26. [CrossRef]
38. Torcunov, A.V.; Baranov, S.A.; Larin, V.S. The internal stresses dependence of the magnetic properties of cast amorphous microwires covered with glass insulation. *J. Magn. Magn. Mater.* **1999**, *196–197*, 835–836. [CrossRef]
39. McHenry, M.E.; Willard, M.A.; Laughlin, D.E. Amorphous and Nanocrystalline Materials for Applications as Soft Magnets. *Prog. Mater. Sci.* **1999**, *44*, 291–433. [CrossRef]
40. Herzer, G. Amorphous and Nanocrystalline Materials. In *Encyclopedia of Materials: Science and Technology*; Elsevier: Amsterdam, The Netherlands, 2001; pp. 149–156. [CrossRef]
41. Talaat, A.; Del Val, J.J.; Zhukova, V.; Ipatov, M.; Klein, P.; Varga, R.; Gonzalez, J.; Zhdanova, M.; Churyukanova, M.; Zhukov, A. Effect of Annealing on Magnetic Properties of Nanocrystalline Hitperm-Type Glass-Coated Microwires. *J. Alloy. Compd.* **2016**, *660*, 297–303. [CrossRef]
42. Vázquez, M.; Hernando, A. A soft magnetic wire for sensor applications. *J. Phys. D. Appl. Phys.* **1996**, *29*, 939–949. [CrossRef]
43. Chiriac, H.; Lupu, N.; Stoian, G.; Ababei, G.; Corodeanu, S.; Óvári, T.A. Ultrathin Nanocrystalline Magnetic Wires. *Crystals* **2017**, *7*, 48. [CrossRef]
44. Zhukova, V.; Corte-Leon, P.; González-Legarreta, L.; Talaat, A.; Blanco, J.M.; Ipatov, M.; Olivera, J.; Zhukov, A. Review of Domain Wall Dynamics Engineering in Magnetic Microwires. *Nanomaterials* **2020**, *10*, 2407. [CrossRef] [PubMed]
45. Zhukov, A.; Shuvaeva, E.; Kaloshkin, S.; Churyukanova, M.; Kostitcyna, E.; Zhdanova, M.; Talaat, A.; Ipatov, M.; Zhukova, V. Studies of interfacial layer and its effect on magnetic properties of glass-coated microwires. *J. Electr. Mater.* **2016**, *45*, 2381–2387. [CrossRef]
46. Mitxelena-Iribarren, O.; Campisi, J.; Martínez de Apellániz, I.; Lizarbe-Sancha, S.; Arana, S.; Zhukova, V.; Mujika, M.; Zhukov, A. Glass-Coated Ferromagnetic Microwire-Induced Magnetic Hyperthermia for in Vitro Cancer Cell Treatment. *Mater. Sci. Eng. C* **2020**, *106*, 110261. [CrossRef]
47. Talaat, A.; Alonso, J.; Zhukova, V.; Garaio, E.; García, J.A.; Srikanth, H.; Phan, M.H.; Zhukov, A. Ferromagnetic Glass-Coated Microwires with Good Heating Properties for Magnetic Hyperthermia. *Sci. Rep.* **2016**, *6*, 1–6. [CrossRef]
48. Kozejova, D.; Fecova, L.; Klein, P.; Sabol, R.; Hudak, R.; Sulla, I.; Mudronova, D.; Galik, J.; Varga, R. Biomedical Applications of Glass-Coated Microwires. *J. Magn. Magn. Mater.* **2019**, *470*, 2–5. [CrossRef]
49. Aronin, A.S.; Abrosimova, G.E.; Kiselev, A.P.; Zhukova, V.; Varga, R.; Zhukov, A. The Effect of Mechanical Stress on $Ni_{63.8}Mn_{11.1}Ga_{25.1}$ Microwire Crystalline Structure and Properties. *Intermetallics* **2013**, *43*, 60–64. [CrossRef]
50. Garcia, C.; Zhukova, V.; Shevyrtalov, S.; Ipatov, M.; Corte-Leon, P.; Zhukov, A. Tuning of Magnetic Properties in Ni-Mn-Ga Heusler-Type Glass-Coated Microwires by Annealing. *J. Alloy. Compd.* **2020**, *838*, 155481. [CrossRef]
51. Zhukov, A.; Ipatov, M.; Corte-León, P.; Gonzalez-Legarreta, L.; Blanco, J.M.; Zhukova, V. Soft Magnetic Microwires for Sensor Applications. *J. Magn. Magn. Mater.* **2020**, *498*, 166180. [CrossRef]
52. Baranov, S.A.; Larin, V.S.; Torcunov, A.V. Technology, Preparation and Properties of the Cast Glass-Coated Magnetic Microwires. *Crystals* **2017**, *7*, 136. [CrossRef]
53. Vázquez, M.; Zhukov, A.P.; Aragoneses, P.; Arcas, J.; Marin, P.; Hernando, A. Magneto-impedance of glass-coated amorphous CoMnSiB microwires. *IEEE Trans. Magn.* **1998**, *34*, 724–728. [CrossRef]
54. Corte-León, P.; Zhukova, V.; Blanco, J.M.; Chizhik, A.; Ipatov, M.; Gonzalez, J.; Fert, A.; Alonso, A.; Zhukov, A. Engineering of Domain Wall Propagation in Magnetic Microwires with Graded Magnetic Anisotropy. *Appl. Mater. Today* **2022**, *26*, 101263. [CrossRef]
55. Zhukova, V.; Cobeño, A.F.; Zhukov, A.; Blanco, J.M.; Larin, V.; Gonzalez, J. Coercivity of glass-coated $Fe_{73.4-x}Cu_1Nb_{3.1}Si_{13.4+}xB_{9.1}$ ($0 \leq x \leq 1.6$) microwires. *Nanostruct. Mater.* **1999**, *11*, 1319–1327. [CrossRef]
56. Goto, T.; Nagano, M.; Wehara, N. Mechanical properties of amorphous $Fe_{80}P_{16}C_3B_1$ filament produced by glass-coated melt spinning. *Trans. JIM* **1977**, *18*, 759–764. [CrossRef]
57. Talaat, A.; del Val, J.J.; Zhukova, V.; Ipatov, M.; Klein, P.; Varga, R.; González, J.; Churyukanova, M.; Zhukov, A. Grain size refinement in nanocrystalline Hitperm-type glass-coated microwires. *J. Magn. Magn. Mater.* **2016**, *406*, 15–21. [CrossRef]
58. Cerqueira, M.F.; Andritschky, M.; Rebouta, L.; Ferreira, J.A.; da Silva, M.F. Macrocrystalline Silicon Thin Films Prepared by RF Reactive Magnetron Sputter Deposition. *Vacuum* **1995**, *46*, 1385–1390. [CrossRef]
59. Srinivas, K.; Manivel Raja, M.; Kamat, S.V. Effect of Partial Substitution of Silicon by Other Sp-Valent Elements on Structure, Magnetic Properties and Electrical Resistivity of Co_2FeSi Heusler Alloys. *J. Alloy. Compd.* **2015**, *619*, 177–185. [CrossRef]
60. Jain, A.; Ong, S.P.; Hautier, G.; Chen, W.; Richards, W.D.; Dacek, S.; Cholia, S.; Gunter, D.; Skinner, D.; Ceder, G.; et al. Commentary: The Materials Project: A Materials Genome Approach to Accelerating Materials Innovation. *APL Mater.* **2013**, *1*, 011002. [CrossRef]
61. Wurmehl, S.; Fecher, G.H.; Ksenofontov, V.; Casper, F.; Stumm, U.; Felser, C.; Lin, H.J.; Hwu, Y. Half-Metallic Ferromagnetism with High Magnetic Moment and High Curie Temperature in Co_2FeSi. *J. Appl. Phys.* **2006**, *99*, 08J103. [CrossRef]
62. Guo, X.B.; Zuo, Y.L.; Cui, B.S.; Li, D.; Yun, J.J.; Wu, K.; Wang, T.; Xi, L. Post Annealing Induced Magnetic Anisotropy in CoFeSi Thin Films on MgO(0 0 1). *J. Phys. D Appl. Phys.* **2017**, *50*, 085006. [CrossRef]

63. Srinivas, K.; Manivel Raja, M.; Sridhara Rao, D.V.; Kamat, S.V. Effect of Sputtering Pressure and Power on Composition, Surface Roughness, Microstructure and Magnetic Properties of as-Deposited Co_2FeSi Thin Films. *Thin Solid Film.* **2014**, *558*, 349–355. [CrossRef]
64. Gunnarsson, K.; Svedlindh, P.; Andersson, J.O.; Nordblad, P.; Lundgren, L.; Aruga Katori, H.; Ito, A. Magnetic Behavior of a Reentrant Ising Spin Glass. *Phys. Rev. B* **1992**, *46*, 8227–8231. [CrossRef] [PubMed]
65. Zagrebin, M.A.; Sokolovskiy, V.V.; Buchelnikov, V.D. Electronic and Magnetic Properties of the Co_2-Based Heusler Compounds under Pressure: First-Principles and Monte Carlo Studies. *J. Phys. D Appl. Phys.* **2016**, *49*, 355004. [CrossRef]
66. Chernenko, V.A.; L'vov, V.A.; Zagorodnyuk, S.P.; Takagi, T. Ferromagnetism of Thermoelastic Martensites: Theory and Experiment. *Phys. Rev. B* **2003**, *67*, 064407. [CrossRef]
67. Zhukov, A.; Ipatov, M.; Del Val, J.J.; Zhukova, V.; Chernenko, V.A. Magnetic and Structural Properties of Glass-Coated Heusler-Type Microwires Exhibiting Martensitic Transformation. *Sci. Rep.* **2018**, *8*, 621. [CrossRef]